Supplementary information

Regenerable photonic aptasensor for detection of bacterial spores with stacks of GaAs-AlGaAs nanoheterostructures

Ishika Ishika[1], Walid M. Hassen[1], René St-Onge[1], Houman Moteshareie[1,2], Azam F. Tayabali[1,2], Jan J. Dubowski[1*]

[1]Interdisciplinary Institute for Technological Innovation (3IT), CNRS IRL-3463, Quantum Semiconductors and Photon-based BioNanotechnology Group, Department of Electrical and Computer Engineering, Université de Sherbrooke, 3000, boul. de l'Université, Sherbrooke, Québec J1K 0A5, Canada.

[2] Biotechnology Laboratory, Environmental Health Science and Research Bureau, Healthy Environments and Consumer Safety Branch, Health Canada, Ottawa, Ontario, Canada.

[*]Address correspondence to

jan.j.dubowski@usherbrooke.ca (submitting author)

Table S1. Examples of regenerable biosensors.

Sensing Approach	**Linker**	**Target**	**Regeneration**	**Regenerable detection concentration**	**Regeneration cycle** **Re-functionalization (Yes/No)**	**Challenges**	**Reference**
SPR biosensor	Dual-His-tagged target protein His-tagged streptavidin or Switchavidin	*E. coli* protein	0.5 M EDTA for 5 min.	3 µM equivalent to 2×10^{10} CFU/mL	2 /Yes	Bulky equipment Loss of sensitivity with higher regeneration cycle	[1]
Localised surface plasmon resonance (LSPR) biosensor	Aptamer	ochratoxin A	Heating in 10% methanol at 70°C for 20 min.	1 nM – 1 µM equivalent to 0.4 µg – 0.4 mg	7/No	Surface roughness increases with greater number of regeneration cycles	[2]

Portable SPR biosensor	Antibody	*Brucella abortus*	10 mM of glycine–HCl pH 2 solution is applied for 5 min.	10^4 CFU/mL	3/Yes	Fraction of whole cell detected	[3]
Fiber biosensor	Aptamer	ochratoxin A	0.5 % SDS (pH 1.9)	200 nM equivalent to 80 µg	300/Yes	Low sensitivity	[4]
Fluorescence biosensor	Cyclodextrins Mannose	*E. coli*	2% SDS at 50oC for 30 min.	10^7 CFU/mL	4/Yes	Low sensitivity and labelling challenges	[5]
Quartz crystal biosensor	Aptamer	*Staphylococcus aureus*	Washing with acetonitrileand acetone	10^5 CFU/mL	10/Yes	Low sensitivity and regeneration procedure is not explained	[6]
Acoustic wave biosensor	Antibody	*E. coli*	pH 2 for 5 min.	10^3 CFU/mL	5/No	Bulky and expensive equipment	[7]
Electrochemical biosensor	Dual bacteria-imprinted polymers	*E. coli* and *S. aureus*	Chemical treatment and heating at 37 ◦C for 10 min.	10^5 CFU/mL	4/No	Low sensitivity	[8]

Electrochemical biosensor	Aptamer	*E. coli* DNA	0.1 M NaOH	10^{-5} μM equivalent to 6.022×10^{9} *E. coli*/mL	3/Yes	Regeneration procedure damaging to aptamers	[9]
Electrochemical biosensor	Aptamer	*B. anthracis toxin*	6 M guanidium hydrochloride for 15 min	100 nM	6/Yes	Low sensitivity and not detecting whole spores	[10]

Table S2. Temporal positions of PL_{max} for the reference and detection runs of *Btk* spores at different concentrations. Errors were calculated based on n-times repeated independent runs.

Concentration of *Btk* spores (CFU/mL)	**0 (Reference)**	**10^3**	**10^4**	**10^5**
1st PL maximum (min)	48.6 ± 1.3 (n= 15)	37.1 ± 0.9 (n=12)	27.3 ± 0.9 (n=9)	18 ± 0.5 (n=9)
2nd PL maximum (min)	40.9 ± 2.1 (n=12)	33.1 ± 1.6 (n=9)	24.5 ± 2.2 (n=9)	15.0 ± 2.1 (n=9)

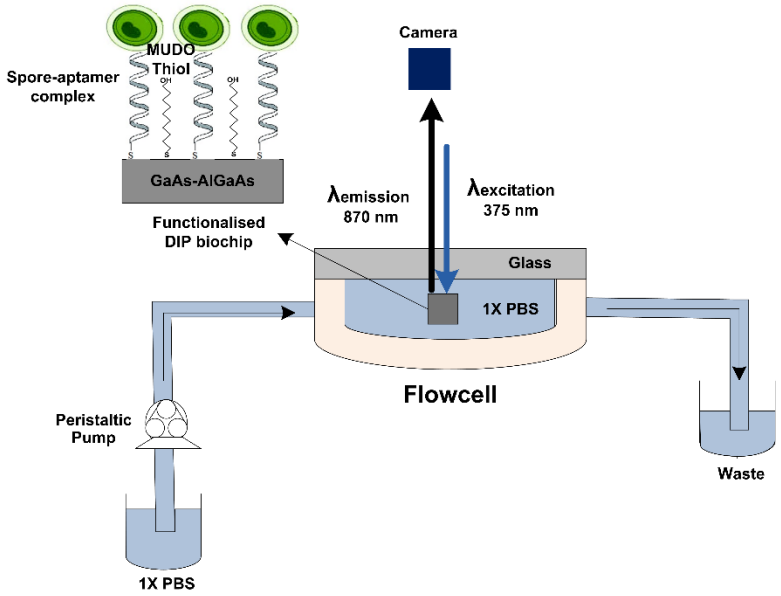

Figure S1. Schematic diagram illustrating the physical sensor prototype for DIP biosensing.

Impact of UV exposure on functionality of aptamers

We did a control by exposing a drop the used aptamer solution (20 µl drop at a concentration of 100 µM) to UV light at 375 nm for 5 minutes (5 minutes largely cover the time of UV irradiation cycled during a whole digital photocorrosion run). After that, UV treated aptamer was used to evaluate the number of captured spores for a tested concentration of 10^5 *Btk* spores/ml. The spore's immobilization number was determined by optical microscopy imaging.

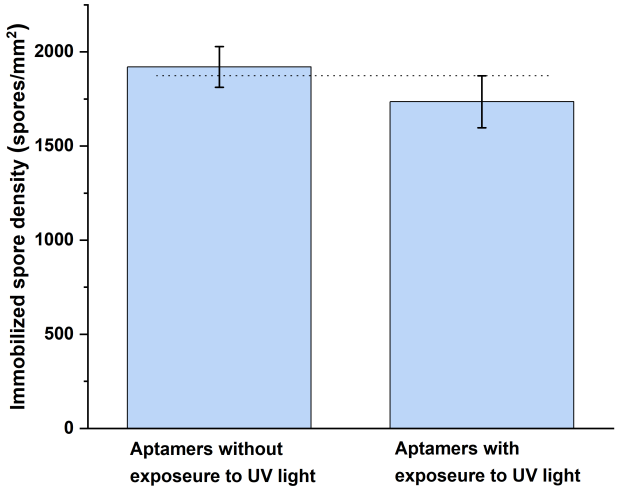

Figure S2. Immobilized spore density on biochip surface for UV treated and non-treated aptamers.

Selectivity of the regenerable DIP biosensor

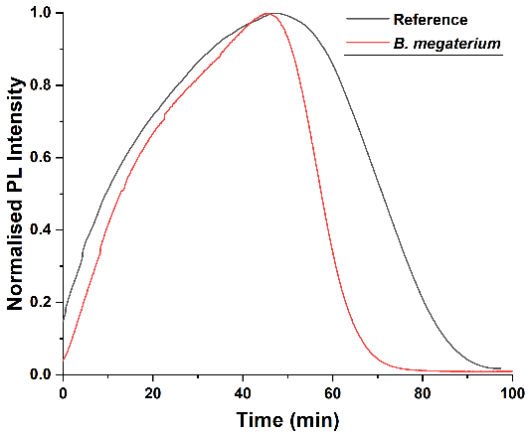

Figure S3. DIP response for biochips exposed to *B. megaterium* at 10^5 CFU/ml concentration.

Regenerable detection of Btk spores collected from Magog River water sample

The 10 ml of real Magog River water was filtered using Millex GV' PVDF membrane filter. The retained matter was washed with 10 mL of DI water. Finally, the filter was backwashed using 10 mL of 1× PBS to collect the suspended matter. The backwashed samples were used as is for reference sample and spiked with *Btk* spores at 10^5 CFU/ml concentration to functionalise detection samples.

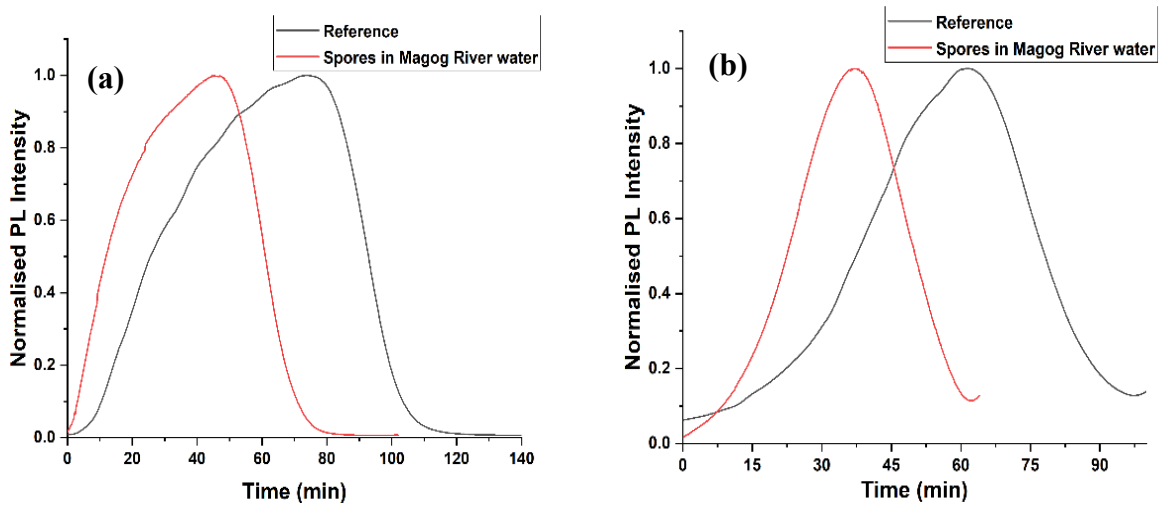

Figure S4. DIP response to spores in the Magog River water at 10^5 CFU/ml concentration for 1st **(a)**, and 2nd **(b)** bilayer.

Surface roughness of DIP biochips

Analysis of the surface morphology of samples was carried out using atomic force microscopy (AFM, Digital Instruments, Nanoscope III). All images were collected in a non-contact mode from 5 µm × 5 µm surface areas with 256 points per line, and at a scan rate of 0.5 Hz. The σ_{rms} was determined as the standard deviation of Z in the given region:

$$\sigma_{rms} = \sqrt{\frac{\sum_{i=1}^{N}(Z_i - Z_{av})^2}{N}} \quad (1)$$

where Z_{av} is the average value of height in the given region, Z_i is the value of Z at each point, and N is the number of points within the given region.

Surface roughness was investigated for a) freshly prepared chips functionalized with 1 mM MUDO thiol and thiolated aptamers against *Btk* spores at 5 µM, and for functionalised chips processed with DIP to remove b) first GaAs-AlGaAs, and c) second pairs of GaAs-AlGaAs nanolayers. The related AFM images are presented in Figure S5.

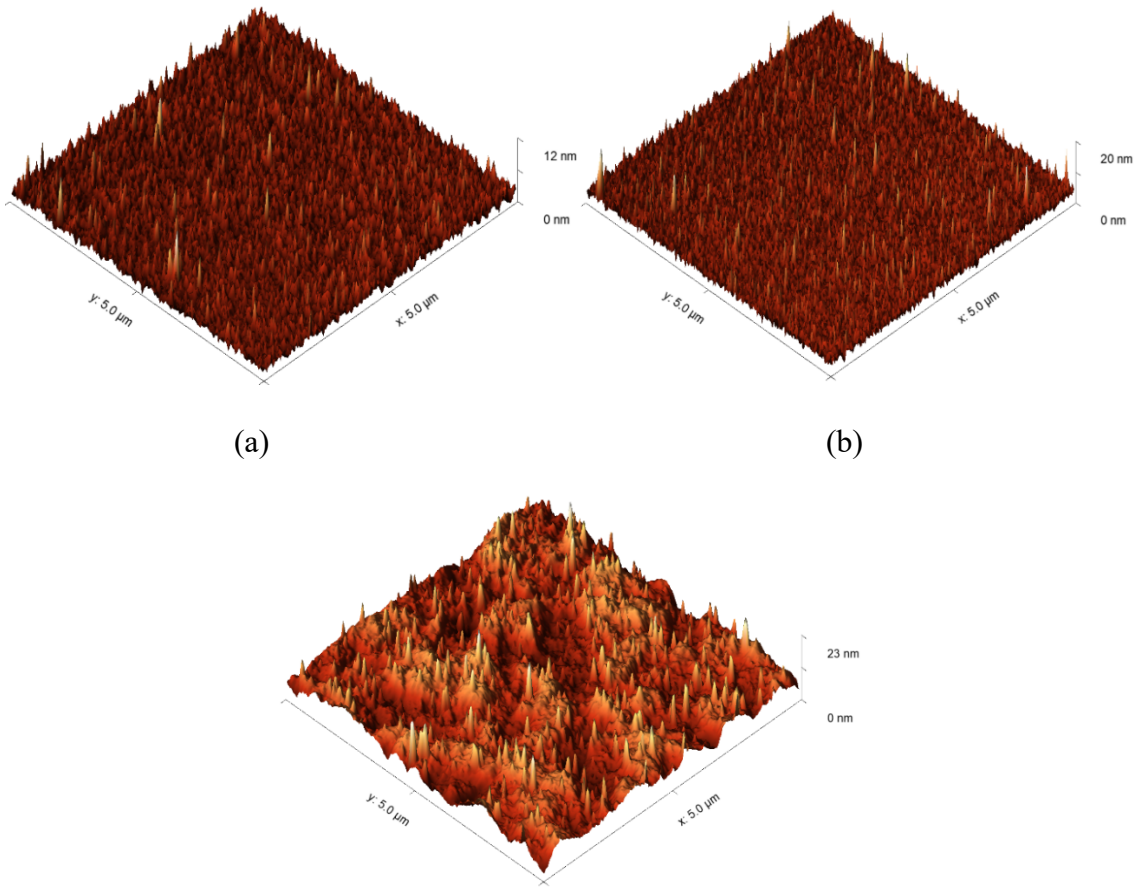

(a) (b)

(c)

Figure S5. AFM surface morphology of a freshly functionalised biochip with MUDO thiol and aptamer against *Btk* spores (a), and after DIP of the first (b) and the second (c) pair of GaAs-AlGaAs nanolayers.

We observed that the average surface roughness of the freshly functionalized biochip, $\sigma_{rms} = 0.81 \pm 0.01$ nm, increased to $\sigma_{rms} = 1.32 \pm 0.03$ nm, and $\sigma_{rms} = 2.12 \pm 0.16$ nm after DIP of the, respectively, first and second pair of the nanolayers.

References

1. A. Gunnarsson, C. J. Stubbs, P. B. Rawlins, E. Taylor-Newman, W.-c. Lee, S. Geschwindner, V. Hytönen, G. Holdgate, R. Jha and G. Dahl, SLAS Discov., 2021, 26, 730-739.

2. J.-H. Park, J.-Y. Byun, H. Mun, W.-B. Shim, Y.-B. Shin, T. Li and M.-G. Kim, Biosens. Bioelectron., 2014, 59, 321-327.

3. L. Pasquardini, N. Cennamo, F. Arcadio, C. Perri, A. Chiodi, G. D'agostino and L. Zeni, Sci. Rep., 2023, 13, 22832.

4. R. Wang, Y. Xiang, X. Zhou, L.-h. Liu and H. Shi, Biosens. Bioelectron., 2015, 66, 11-18.

5. Y. Qu, T. Wei, W. Zhan, C. Hu, L. Cao, Q. Yu and H. Chen, J. Mater. Chem. B, 2017, 5, 444-453.

6. Y. Lian, F. He, H. Wang and F. Tong, Biosens. Bioelectron., 2015, 65, 314-319.

7. J. Chawich, W. M. Hassen, C. Elie-Caille, T. Leblois and J. J. Dubowski, Biosensors, 2021, 11, 145.

8. X. Xu, X. Lin, L. Wang, Y. Ma, T. Sun and X. Bian, Biosensors, 2023, 13, 868.

9. E. Yuhana Ariffin, L. Y. Heng, L. L. Tan, N. H. Abd Karim and S. A. Hasbullah, Sensors, 2020, 20, 1279.

10. L. N. Cella, P. Sanchez, W. Zhong, N. V. Myung, W. Chen and A. Mulchandani, Anal. Chem., 2010, 82, 2042-2047.